ELSEVIER
International Journal of Mass Spectrometry 216 (2002) 155–168
International Journal of Mass Spectrometry
www.elsevier.com/locate/ijms

The generation of gaseous $[Co_xO_y]^-$ clusters and their reactions with alcohols: formation of homoleptic cobalt alkoxides $[Co_4(OR)_8]^-$

Ma Nu Yi, Keith J. Fisher, Ian G. Dance*

School of Chemistry, University of New South Wales, Sydney 2052, Australia

Received 21 August 2001; accepted 16 January 2002

Abstract

Laser ablation of Co_3O_4 yielded 26 gaseous anions $[Co_xO_y]^-$ ranging from $[CoO_2]^-$ to $[Co_{13}O_{14}]^-$, and $[Co(OH)_3]^-$, which were detected and investigated using Fourier transform ion cyclotron resonance–mass spectrometry (FT-ICR–MS). $[CoO_2]^-$, $[Co_2O_3]^-$, and $[Co_4O_4]^-$ were the more abundant products. The clusters occur mainly in two series, $[Co_xO_x]^-$ and $[Co_xO_{x+1}]^-$, with the equiatomic ions more abundant for each x. This series, extending previous observations, supports a pattern of electron population for $[M_xO_y]^-$ clusters that is different from the general electron population for analogous $[M_xS_y]^-$ clusters. Collision-induced dissociation and some density functional calculations support an extended structure for $[OCoO]^-$ and a cubanoid structure for $[Co_4O_4]^-$. The principal reaction of $[CoO_2]^-$ with methanol, ethanol and 2-propanol is dehydrogenation and formation of $[CoO_2H]^-$ and $[CoO_2H_2]^-$. The less oxidising $[Co_4O_4]^-$ undergoes a series of reactions involving: (a) ROH addition, coupled with (b) ROH addition plus H_2O elimination (with (b) faster than (a)), through a series of intermediates, culminating in $[Co_4(OR)_8]^-$ with the proposed structure $(\mu_3\text{–OR})_4(\text{Co–OR})_4$. Structurally consistent mechanisms are outlined. This formation of homoleptic metal alkoxides is more favourable than alcohol condensation to form ethers, or alcohol oxidation, and it is postulated that other non-oxidising $[M_xO_y]^-$ clusters may also form gaseous homoleptic metal alkoxides. Some slower homologation of coordinated methoxide to coordinated ethoxide is evident in the reactions with methanol. (Int J Mass Spectrom 216 (2002) 155–168) © 2002 Elsevier Science B.V. All rights reserved.

Keywords: Cobalt oxide; Anions; Alcohols; Reactions; Alkoxides; Laser ablation; Collision-induced dissociation; Fourier transform ion cyclotron resonance–mass spectrometry

1. Introduction

We are investigating the formation of metal–element clusters M_xE_y ($E = O, S, P$) in the gas phase, and their properties and reactions [1]. Our research concentrates on anionic clusters $[M_xE_y]^-$ [2–4], which are less common than the corresponding cations that have been frequently studied. These $[M_xE_y]^-$ anions are less oxidising, more basic, and more nucleophilic than cations. In this paper, we focus on some cobalt oxide anions, and their reactions with alcohols, investigated by Fourier transform ion cyclotron resonance–mass spectrometry (FT-ICR–MS).

The literature contains reports of investigations of relevant anions, including Co^- reacting with thiols [5], the generation of clusters $[CrO_3]^-$ [6], $[(CrO_3)_n]^-$ [7],

---

* Corresponding author. E-mail: i.dance@unsw.edu.au

1387-3806/02/$ – see front matter
PII S1387-3806(02)00582-1

$[M(CO)_nO_m]^-$ (M = Fe, Cr, Mo, Mn, Co) ($n = 0$–4, $m = 4, 5$) [8], and (M = Ni, Fe, Cr, W, Mo, V; $y = 2$–5) [9]. There was a very brief report of the formation of $[Co_xO_y]^-$ clusters, produced by laser vaporisation of CoO and Co_3O_4, and their reactions with small hydrocarbons [10]. More recently, Almoster-Ferreira and coworkers [11] have reported the formation of $[Co_xO_y]^-$ anions by laser ablation, and the reactions of $[CoO_2]^-$ and $[Co_2O_3]^-$ with methanol. Other investigations relevant here include the FT-ICR–MS of $[MnO_x]^-$ $x = 2, 3, 4$, and the reactions of $[MnO_2]^-$ and $[MnO_3]^-$ with aliphatic alcohols [12,13]; the formation of $[Nb_xO_y]^-$ clusters by laser ablation and reactions of some of them with methanol and ethanol [14]; and the catalytic reaction cycles in which $[Mo_2O_7]^{2-}$ and $[(cat)Mo_2O_7]^-$ oxidise primary alcohols in the gas phase [15].

In this paper, we report a wider range of anionic $[Co_xO_y]^-$ clusters formed by laser ablation of Co_3O_4, the collision-induced dissociation of the more abundant species, and the reactions of $[CoO_2]^-$ and $[Co_4O_4]^-$ with methanol, ethanol, and 2-propanol representing primary and secondary alcohols. For comparison, one thiol, *n*-propanethiol, was included in the investigation. Since the reaction pathways could involve alcohol coupling to form ethers (possibly bound), and alcohol oxidation, the possible products diethylether and acetone were also investigated as reactants with $[CoO_2]^-$ and $[Co_4O_4]^-$. Other reactants that could provide information about reactivities and the reactions were D_2O, H_2S for comparison with RSH, and N_2O as O atom source.

2. Experimental

Co_3O_4 was prepared from precipitated $CoCO_3$ (obtained by treating aqueous $Co(NO_3)_2$ with aqueous Na_2CO_3 in the absence of air) by heating for 1 h at 700 °C. The synthetic Co_3O_4 was ionised by laser ablation with a 8 ns pulse from a Nd-YAG laser (1064 nm, Spectra Physics DCR-11) focused to an area of 0.4 mm diameter. The laser power from $\sim 6 \times 10^2$ to 5×10^3 MW cm^{-2} in a Q-switched mode was applied for the ion generation and their reactions. The ions generated by the pressed sample in the ICR cell were then detected and their spectra obtained by a Spectrospin CMS-47 FT-ICR–MS equipped with a 4.7 T superconducting magnet. Details of this technique were described previously [2]. The product ions were observed with time delays between ionisation and acquisition of 0.01–0.1 s. Mass windows were scanned from ∼20 to 1000 *m*/*z*.

Collision-induced dissociation (CID) experiments or ion/molecule reactions were performed with the selected ions and the Ar collision gas or the reactant gas or vapour from a volatile liquid at $\sim 1 \times 10^{-5}$ Pa. The gas or vapour reactant for ion/molecule reactions was allowed to pass from the heated gas inlet through a molecular leak valve into the UHV region. The ion of interest was isolated in the cell by ejecting all the unwanted ions using a double resonance ejection pulse, followed by an acceleration pulse of 10–50 μs. Collision delays were varied from 0.01 to 0.1 s before pre-acquisition excitation and subsequent detection, whereas reaction delays for ion/molecule reactions were from 1 to 100 s.

3. Results and interpretations

3.1. LA–FT-ICR–MS of synthetic Co_3O_4

Synthetic Co_3O_4 generated 26 gaseous binary anions of the type $[Co_xO_y]^-$ ($x = 1$–13, $y = 2$–14), together with $[Co(OH)_3]^-$ presumably due to trace water contamination. Our spectrum of species formed up to *m*/*z* 500 is very similar to that previously published [11], but we were able to observe an additional 15 $[Co_xO_y]^-$ clusters at higher mass. All of the product anions we observed are listed in Table 1.

The compositions of the $[Co_xO_y]^-$ clusters are graphed in Fig. 1, which shows the pattern of two principal compositions, $[Co_xO_x]^-$ $x = 2$–13, and $[Co_xO_{x+1}]^-$ $x = 1$–13. Only one species, $[Co_7O_6]^-$, was metal rich. The most abundant ions were $[CoO_2]^-$ and $[Co_4O_4]^-$, while $[Co_2O_3]^-$ was

Table 1
Negative ions generated by laser ablation of Co_3O_4

Mass (U)	Formula	Relative intensity (%)
91	CoO_2	100
110	$Co(OH)_3$	25
150	Co_2O_2	9
166	Co_2O_3	70
225	Co_3O_3	22
241	Co_3O_4	15
300	Co_4O_4	99
316	Co_4O_5	8
375	Co_5O_5	25
391	Co_5O_6	10
450	Co_6O_6	9
466	Co_6O_7	6
509	Co_7O_6	Trace
525	Co_7O_7	3
541	Co_7O_8	Trace
599	Co_8O_8	4
615	Co_8O_9	Trace
674	Co_9O_9	5
690	Co_9O_{10}	Trace
749	$Co_{10}O_{10}$	4
765	$Co_{10}O_{11}$	6
824	$Co_{11}O_{11}$	6
840	$Co_{11}O_{12}$	7
899	$Co_{12}O_{12}$	Trace
915	$Co_{12}O_{13}$	Trace
974	$Co_{13}O_{13}$	Trace
990	$Co_{13}O_{14}$	Trace

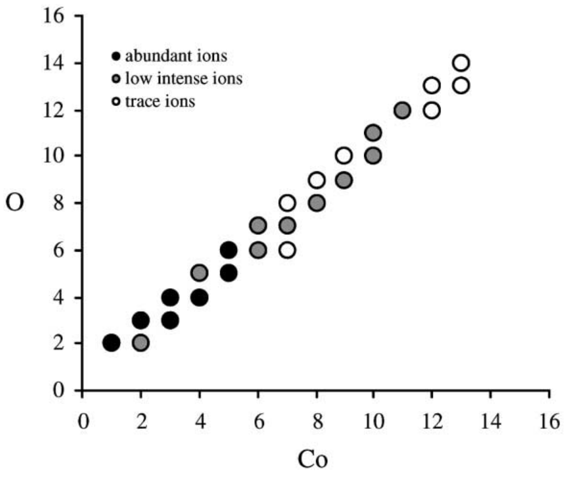

Fig. 1. Composition map of the $[Co_xO_y]^-$ clusters produced by the laser ablation of synthetic Co_3O_4.

also prominent. Equiatomic $[Co_xO_x]^-$ ions were generally more abundant than $[Co_xO_{x+1}]^-$ for all x except 2.

3.2. Collision-induced dissociation of $[Co_xO_y]^-$ clusters

CID of four $[Co_xO_y]^-$ ions, $(x, y) = (2, 3), (3, 3), (4, 4), (5, 5)$, was effected, using argon as collision gas. The results are presented in Table 2, together with speculation about the unobserved neutral species lost. $[CoO_2]^-$ was an abundant product in all cases. The CID of $[Co_2O_3]^-$ is consistent with the connectivity $[O–Co–O–Co–O]^-$. CID of $[Co_5O_5]^-$ yielded both $[CoO_2]^-$ and $[Co_4O_4]^-$, the two most prominent ions in the original laser ablation, further indicating the enhanced stability of these two cluster anions.

3.3. Structures of $[CoO_2]^-$ and $[Co_4O_4]^-$

Density functional (DF) calculations with gradient corrections (BLYP) and numerical basis sets, in the program DMol [16], have been applied to $[CoO_2]^-$ and $[Co_4O_4]^-$. These indicate that the structure of $[CoO_2]^-$ is probably linear, but with a very soft bending potential, and that the electron affinity of $[CoO_2]$ is high, ca. 2.9 eV. For $[Co_4O_4]^-$ a cubane structure **1** would be expected, by analogy with other M_4E_4 clusters in the gas and condensed phases: the DF calculations show that the electronic structure of cubanoid $[Co_4O_4]^-$ is complex, with close-lying electronic states, and is strongly linked to tetrahedral distortions which change the $Co \cdots Co$ distances. A planar structure **2** with lesser co-ordination of Co but short Co–Co bonds is calculated to be energetically competitive with **1** for anionic $[Co_4O_4]^-$, but not as the neutral species. We note that the appearance of $[Co_3O_3]^-$ in the CID of $[Co_4O_4]^-$ is more consistent with the cubane structure **1** than the planar square structure **2**, and the cubanoid structure is assumed for further analysis of the reaction patterns. The DF calculations show that $[Co_4O_4]^-$ is a particularly electron-rich species, with low ionisation energy and

Table 2
Dissociations of $[Co_xO_y]^-$ ions induced by collision with Ar

Parent ion	Fragment products observed from CID	
	Anions $[Co_xO_y]^-$ (relative intensity)	Neutral losses[a]
$[Co_2O_3]^-$	CoO (8), CoO_2 (100), Co_2O_2 (8)	CoO, *CoO_2*, *O*
$[Co_3O_3]^-$	CoO (5), CoO_2 (28), Co_2O_2 (20), Co_2O_3 (25)	Co_2O, *Co*, *CoO*, *Co_2O_2*
$[Co_4O_4]^-$	CoO_2 (35), Co_2O_2 (15), Co_2O_3 (30), Co_3O_3 (25)	Co_3O_2, *Co_2O*, *CoO*, *Co_2O_2*
$[Co_5O_5]^-$	CoO_2 (25), Co_4O_4 (30)	CoO, *Co_4O_3*

[a] Based on the major fragment product (plain) and the minor fragments (italic, in decreasing order of the intensities of fragment products).

high energy filled orbitals. This is consistent with the reactivity:

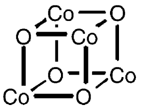

1

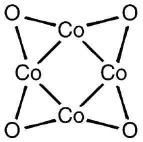

2

3.4. Reactions of $[CoO_2]^-$ with alcohols

Details of these reactions are presented in Table 3. For methanol, ethanol and 2-propanol a first hydrogenation to form $[CoO_2H]^-$ occurred very rapidly, followed by fast second hydrogenation to form $[CoO_2H_2]^-$ which was the dominant product for the remainder of the reaction period. The intermediate $[CoO_2H]^-$ was not reported by Almoster-Ferreira and coworkers [11], probably because it rapidly adds a second hydrogen atom to form $[CoO_2H_2]^-$. In our experiments the reactive monohydrogenated intermediate $[CoO_2H]^-$ is present only within 2 s, at $\leq 15\%$ relative intensity, but it is formed with all three alcohols (Table 3). The structure of $[CoO_2H_2]^-$ is probably $[HOCoOH]^-$. Notable from Table 3 is the formation of $[CoO_2H_3]^-$ by ethanol and propanol, with the implied structure $[HOCo(OH_2)]^-$ containing water, and the formation by all three alcohols of traces

Table 3
The anionic products formed by the reactions of $[CoO_2]^-$ with CH_3OH, C_2H_5OH, 2-C_3H_7OH

CH_3OH				C_2H_5OH				2-C_3H_7OH			
Time (s)	Mass	Intensity[a]	Formula(e)[b]	Time (s)	Mass	Intensity[a]	Formula(e)[b]	Time (s)	Mass	Intensity[a]	Formula(e)[b]
1–50	32	5	O_2/CH_3OH	1–50	32	5	O_2/CH_3OH	1–50	32	25	*O_2/CH_3OH*
1–50	35	12	*H_3O_2*	1–50	35	30	*H_3O_2*	1–50	35	17	*H_3O_2*
				1–10	45	20	*C_2H_5O*	1–30	59	18	*C_3H_7O/Co*
1–2	92	15	*CoO_2H*	1–2	92	10	CoO_2H	1–2	92	10	CoO_2H
2–50	93	100	**CoO_2H_2**	2–50	93	100	**CoO_2H_2**	2–50	93	100	**CoO_2H_2**
2–10	106	5	CoO_2CH_3	3–50	94	15	*CoO_2H_3*	4–50	94	30	*CoO_2H_3*
1–50	107	<5	CoO_3/CoO_2CH_4	3–50	107	5	CoO_3	4–50	107	5	CoO_3
3–10	108	<5	CoO_3H/CoO_2CH_5								
3–10	109	<5	CoO_3H_2/CoO_2CH_6	2–50	109	13	CoO_3H_2	4–50	109	6	CoO_3H_2
				2–50	119	5	$CoO_2C_2H_4$	5–50	133	7	$CoO_2C_3H_6$
				2–5	120	5	$CoO_2C_2H_5$				
				3–5	122	5	$CoO_2C_2H_7$				
5–50	122	<5	$CoO_3CH_3/CoO_2C_2H_7$	3–10	137	5	$CoO_3C_2H_6$	6–10	151	5	$CoO_3C_3H_8$
15–50	136	<5	$CoO_3C_2H_5/CoO_2C_3H_9$	3–50	150	8	$CoO_2C_4H_{11}$	6–10	178	10	$CoO_2C_6H_{15}$
				3–50	165	12	*$CoO_3C_4H_{10}$*	7–50	193	20	*$CoO_3C_6H_{14}$*
15–50	152	<5	$CoO_3C_3H_9/CoO_2C_4H_{13}$	4–50	194	4	$CoO_3C_6H_{15}$	8–50	236	5	$CoO_3C_9H_{21}$
15–50	166	<5	$CoO_3C_4H_{11}/CoO_2C_5H_{15}$								

[a] Maximum relative ion intensity (%) at any stage.

[b] Major products are bold; minor products italicised; plain text signifies trace products.

of $[CoO_3]^-$ through oxygenation. In the reactions with methanol there were ambiguities in identification of trace products due to the mass equivalence $CH_4 \equiv O$ [17], but the identification of product ions incorporating the alcohols could be made unambiguously from the reactions with ethanol and propanol. From Table 3 it is then evident that (a) the products $[OCo(OR)_2]^-$ and $[Co(OR)_3]^-$ are present for all three alcohols over long-time periods; (b) the species $[OCo(OH)(OR)]^-$ for R = Et and 2-Pr occur at intermediate times, and (c) $[CoO_2(R–H)]^-$ for R = Et and 2-Pr occurs throughout the reaction. All of the alkoxide products occur with low intensity (Table 3). The previous investigation with methanol only [11] was not able to detect these additional species which reveal that $[CoO_2]^-$ is able to form metal alcoxides as well as cause oxidative dehydrogenation of alcohols.

3.5. Reactions of $[Co_4O_4]^-$ with alcohols

Reactions of $[Co_4O_4]^-$ with methanol, ethanol and 2-propanol generate a rich set of products, many of which are abundant. Details of the products observed are presented in Table 4, and Fig. 2 shows representative spectra for the reaction of $[Co_4O_4]^-$ with 2-propanol. The relative reaction rates of $[Co_4O_4]^-$ with methanol, ethanol and 2-propanol decrease in the order 2-propanol > ethanol > methanol.

The products observed for all three alcohols follow a single pattern involving addition of ROH and elimination of H_2O. Scheme 1 provides a generalised representation of these products, and it is evident that the two processes involved are (a) addition of ROH (dotted arrows in Scheme 1), and (b) addition of ROH with concomitant elimination of H_2O (solid arrows). The eventual effect of these reaction sequences is conversion of $[Co_4O_4]^-$ to $[Co_4(OR)_8]^-$, which is observed for all three alcohols, and becomes the most intense product ion for R = Me and Et. The final formation of $[Co_4(O–2–Pr)_8]^-$ is a little slower than for the other alcohols, which is the reason why it does not become the most abundant species during the time (100 s) of our reactions. There is no evidence for further reaction of $[Co_4(OR)_8]^-$, except for $[Co_4(OMe)_8]^-$ as described above. Not all of the products shown in Scheme 1 are prominent for all three alcohols: specifically, the ions $[Co_4O_2(OR)_2(OH)_2]^-$,

Table 4
Product anions common to the reactions of $[Co_4O_4]^-$ with CH_3OH, C_2H_5OH and $2\text{-}C_3H_7OH$

Product anions (R = CH_3, C_2H_5, or C_3H_7)	Reactions of $[Co_4O_4]^-$					
	CH_3OH		C_2H_5OH		$2\text{-}C_3H_7OH$	
	Time (s)[a]	Intensity[b]	Time (s)[a]	Intensity[b]	Time (s)[a]	Intensity[b]
$Co_4O_3(OR)(OH)$	5–40	20	4.5–60	8	4–80	13
$Co_4O_3(OR)_2$	6–40	22	4.5–50	15	5–60	13
$Co_4O_2(OR)_2(OH)_2$	10–50	14			6–35	10
$Co_4O_2(OR)_3(OH)$	11–50	13	7–45	10	6–60	15
$Co_4O(OR)_3(OH)_3$	11–50	12				
$Co_4O_2(OR)_4$	11–50	9	9–35	6	9–80	10
$Co_4O(OR)_4(OH)_2$	10–70	20	20–30	5	8–80	20
$Co_4(OR)_4(OH)_4$	15–60	10				
$Co_4O(OR)_5(OH)$	11–80	28	9–45	10	8–60	35
$Co_4O(OR)_6$	11–80	24	9–50	32	11–55	48
$Co_4(OR)_5(OH)_3$	15–30	35	25–40	5	9–100	30
$Co_4(OR)_6(OH)_2$	20–80	48	20–55	15	13–100	75
$Co_4(OR)_7(OH)$	20–60	85	20–70	100	15–100	100
$Co_4(OR)_8$	30–80	100	20–70	100	30–100	15

[a] Time period during which the product anion was observable.
[b] Maximum intensity (%) of the product anion at any stage in the reaction.

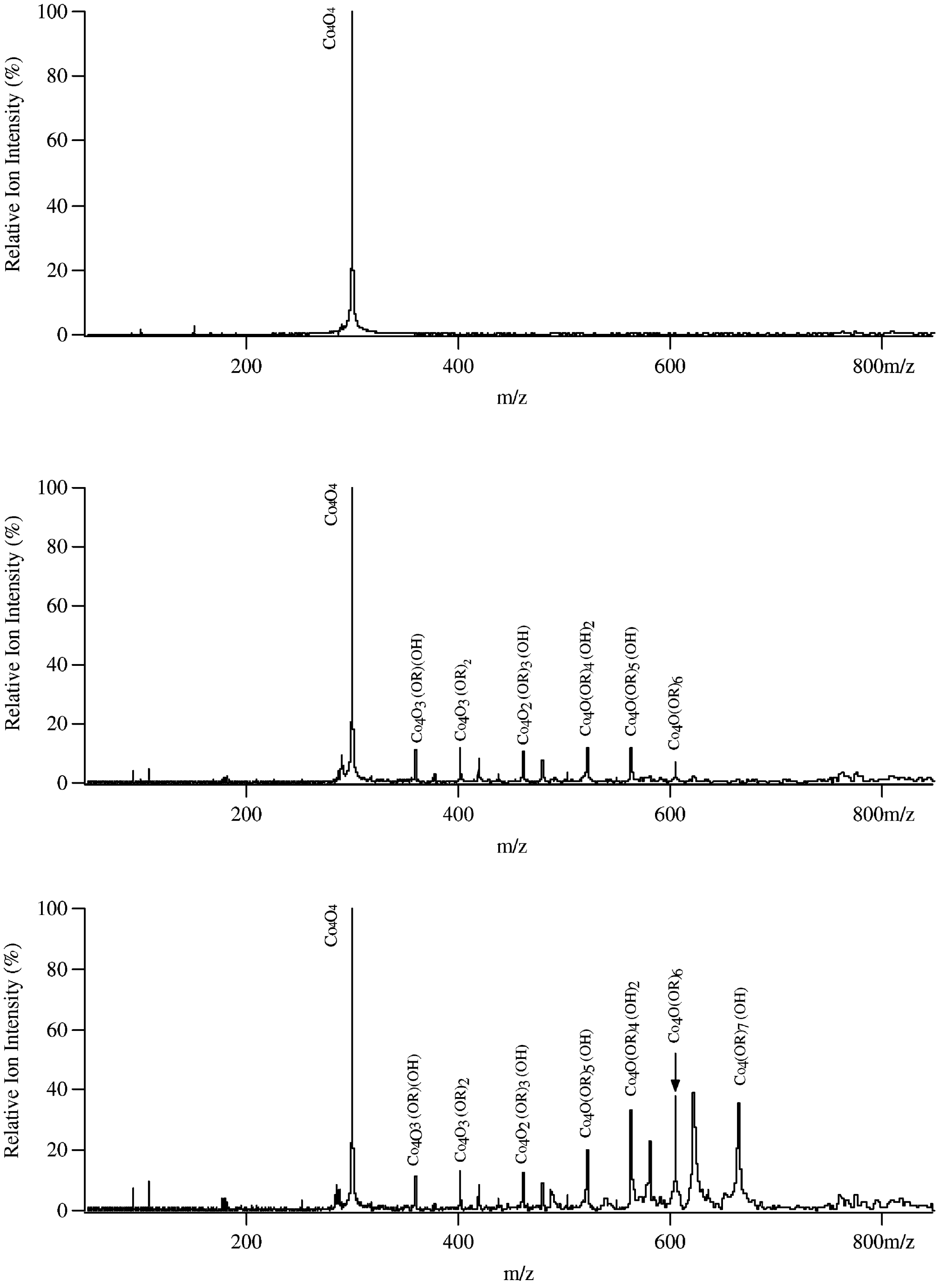

Fig. 2. FT-ICR spectra of the products of the reaction of $[Co_4O_4]^-$ and 2-propanol after reaction periods of 0 s (top), 13 s (middle) and 21 s (bottom).

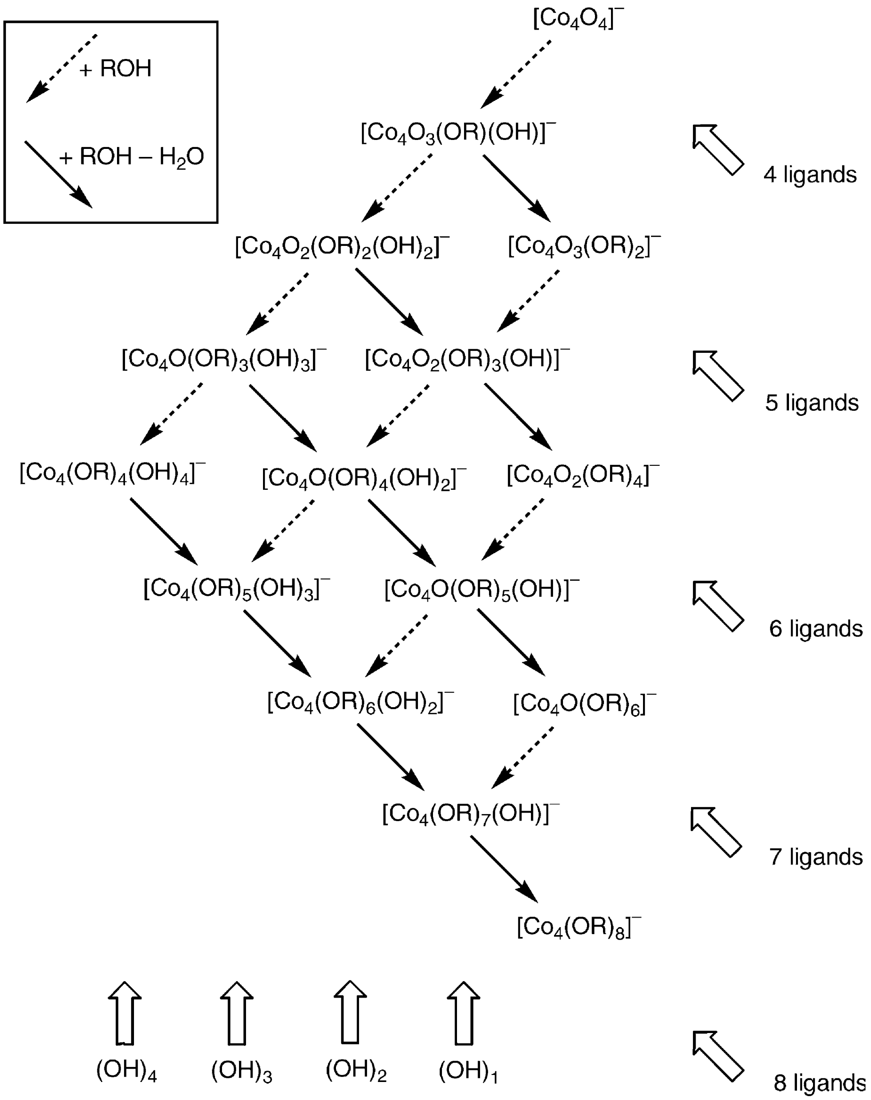

Scheme 1. Generalised scheme for the reactions of $[Co_4O_4]^-$ with alcohols ROH: R = CH_3, C_2H_5, $CH(CH_3)_2$.

$[Co_4O(OR)_3(OH)_3]^-$ and $[Co_4(OR)_4(OH)_4]^-$ are very weak or absent for R = Et, 2-Pr.

The times of appearance and the relative abundances of the products reveal the relative rates of the processes competing at the intermediate stages. Scheme 2 shows the times of initial appearance of the intermediates for the reaction with methanol, which is the most informative. There are several notable features of these reactions. First, the times indicate that horizontal processes in the chart, that is elimination of H_2O without addition of alcohol, do not occur. Second, the concomitant addition of alcohol and elimination of water (solid arrows) is generally faster than addition of alcohol (dotted arrows). Third, all of the intermediates in the centre of the chart are relatively reactive, consistent with their general low abundance. The later intermediates $[Co_4O(OMe)_6]^-$ and $[Co_4(OMe)_7(OH)]^-$ are abundant due to their slower

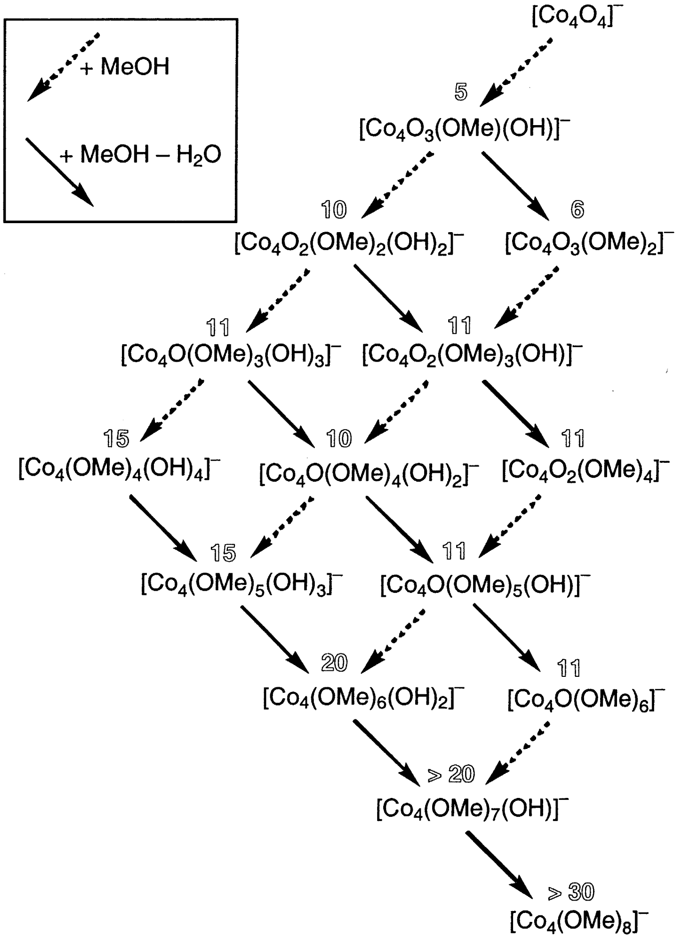

Scheme 2. Times (s, outline font) for first appearance of intermediates in the reaction of $[Co_4O_4]^-$ with methanol. Note that in all except the final reactions the addition of MeOH with elimination of H_2O is relatively fast.

reactions to $[Co_4(OMe)_8]^-$. The reason for the low intensity of the intermediates $[Co_4O_2(OR)_2(OH)_2]^-$, $[Co_4O(OR)_3(OH)_3]^-$ and $[Co_4(OR)_4(OH)_4]^-$ for ethanol and propanol is their rapid reaction by alcohol addition and concomitant water elimination. The fully added intermediate $[Co_4(OR)_4(OH)_4]^-$ is reached only with methanol.

There is a possible alternative formulation of the products, involving coordinated ether ROR formed by elimination of water: $2OR \equiv ROR + O$ (not changing the number of ligands). Diethyl ether was found not to react with or bind to $[Co_4O_4]^-$, and since the ligating ability of ethers is normally very much less than that of alkoxides, we reject such formulations. The generally consistent formulation in Scheme 1 is believed to be correct.

Straight-forward mechanisms can be written for the two fundamental process of ROH addition (Fig. 3(a)) and ROH addition plus H_2O elimination (Fig. 3(b)).

Processes (a) and (b) can continue, through intermediates such as $Co_4O(OR)_5(OH)$ (Table 4) with structures such as **3**. Note that the mechanism of sequential $\{(a) + (b)\}$ (Fig. 3) leads to location of OR groups equally on Co and at the triply bridging vertices of

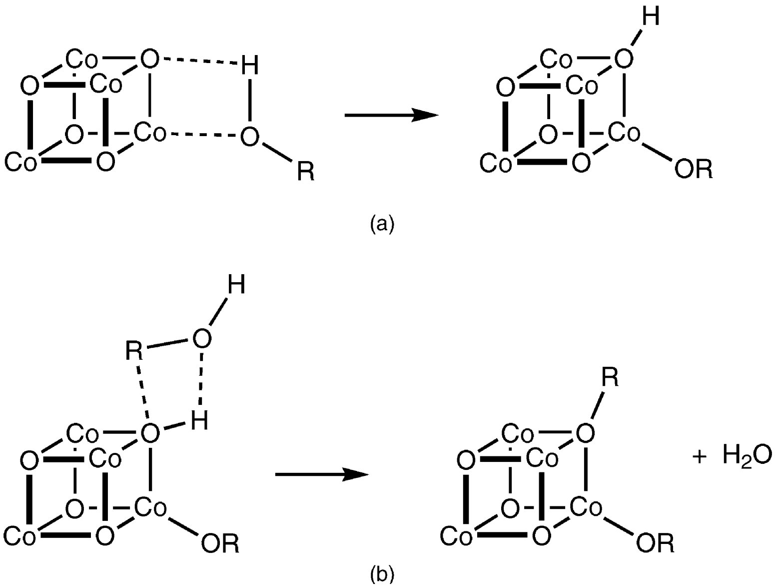

Fig. 3. (a) Transition state for the collision and addition of ROH to a Co–O bond of $[Co_4O_4]^-$; (b) mechanism for addition of ROH to an O–H bond of the $[Co_4O_{4-n}(OH)_n]^-$ core, with elimination of H_2O. In both cases opposite polarities are juxtaposed in the transition state. Process (b) is generally faster than process (a).

the cube, which accounts for the connectivity of **3**. Note that regio-isomers are possible for some intermediates, such as variation of the *trans*-(μ_3–O) and unligated Co in **3**. This sequence of reactions is restricted to a total of eight ligands associated with the Co_4 core, as emphasised in Scheme 1, and completes at the formation of $[Co_4(OR)_8]^-$, with the structure $(\mu_3\text{–}OR)_4(Co\text{–}OR)_4$ (**4**).

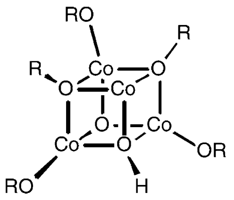

$Co_4O(OR)_5(OH)$ **3**

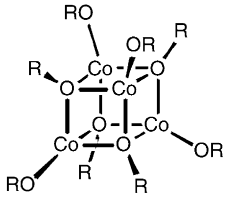

$(\mu_3\text{-}OR)_4(Co\text{-}OR)_4$ **4**

The absence of water elimination from two μ_3–OH, already noted as an absence of horizontal arrows in Scheme 1, is consistent with the cubanoid structure because such μ_3–OH groups are located across a face-diagonal of the cube and are directed away from each other.

In the reaction of $[Co_4O_4]^-$ with methanol, three additional products were observed at high mass and at long time periods. These products, which were low intensity, are listed in Table 5. Their compositions correspond to the final product $[Co_4(OCH_3)_8]^-$ plus CH_2, $(CH_2)_2$, and $(CH_2)_3$, and so appear to represent the conversion of methoxide to ethoxide and formation of $Co_4(OCH_3)_7(OC_2H_5)$, $Co_4(OCH_3)_6(OC_2H_5)_2$, and $Co_4(OCH_3)_5(OC_2H_5)_3$ at long times. Alternative but less feasible formulations are listed in Table 5. A probable transition state for the collision and reaction of CH_3OH with an $–OCH_3$ section of $[Co_4(OCH_3)_8]^-$ is shown in Fig. 4(a), leading to elimination of H_2O and formation of $–OCH_2CH_3$. Fig. 4(b), a space-filling representation of $[Co_4(OCH_3)_8]^-$, shows the exposure of the CH_3 groups of both the $Co_3(\mu_3\text{–}OCH_3)$ and $Co\text{–}OCH_3$ functions, and the geometrical feasibility of this reaction. The non-observation of this secondary reaction type with ethanol and 2-propanol is explained by the greater steric crowding involved, and lesser polarisation of the α-CH_2 of the bound alkoxide.

Table 5
Additional low intensity product anions formed in the reaction of $[Co_4O_4]^-$ with CH_3OH

Mass	Time (s)[a]	Probable[b] and possible compositions	Probable formula
497	>30–80	**$Co_4O_8C_9H_{26}$** $Co_4O_7C_{10}H_{30}$, $Co_4O_6C_{11}H_{34}$, $Co_4O_9C_8H_{22}$	$Co_4(OCH_3)_7(OC_2H_5)$
511	>30–80	**$Co_4O_8C_{10}H_{28}$** $Co_4O_7C_{11}H_{32}$, $Co_4O_6C_{12}H_{36}$, $Co_4O_9C_9H_{24}$	$Co_4(OCH_3)_6(OC_2H_5)_2$
525	>30–80	**$Co_4O_8C_{11}H_{30}$** $Co_4O_7C_{12}H_{34}$, $Co_4O_6C_{13}H_{38}$, $Co_4O_9C_{10}H_{26}$	$Co_4(OCH_3)_5(OC_2H_5)_3$

[a] Time period during which the product anion was observable.
[b] Bold entries represent probable composition.

3.6. Reactions of $[CoO_2]^-$ and $[Co_4O_4]^-$ with n-propanethiol and acetone

In the reaction of $[Co_4O_4]^-$ with *n*-propanethiol, $[C_3H_7S]^-$ was the most abundant product, generated by proton transfer: the mass of C_3H_7S is the same as that of CoO, but a number of mass spectrometric observations discounted the formation of $[CoO]^-$ by reaction of $[Co_4O_4]^-$ with C_3H_7SH. Other low intensity products were $[HS]^-$, $[H_3S]^-$, $[S_2]^-$, and the $[Co_4O_4]^-$ related ions $[Co_4O_{4-x}S_x]^-$ ($x = 1$–4), $[Co_4O_4S_x]^-$ ($x = 1, 2$), and $[Co_4O_{4-x}S_{x+1}]^-$ ($x = 1, 2$). Addition of *n*-C_3H_7SH to $[Co_4O_4]^-$ was not observed, in contrast to the reactions with alcohols. Reaction of $[CoO_2]^-$ with acetone produced only $[C_3H_5O]^-$ and $[CoO_2H]^-$ via H transfer. The most intense ion formed in the reaction of acetone with $[Co_4O_4]^-$ was $[C_3H_5O]^-$, indicating the basicity of $[Co_4O_4]^-$.

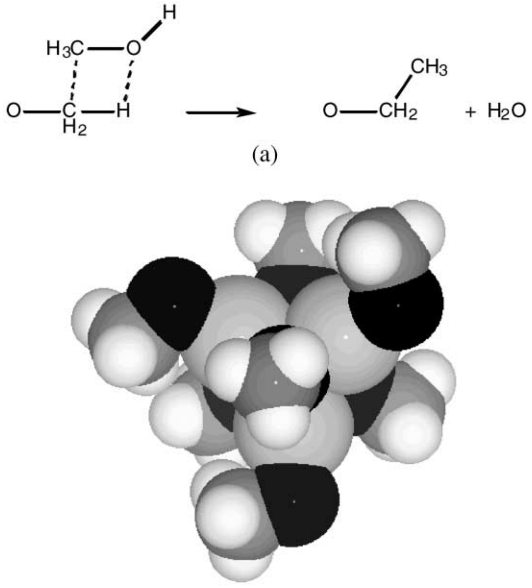

(a)

(b)

Fig. 4. (a) Transition state for addition of CH_3–OH to a μ_3–OCH_3 function, forming μ_3–OCH_2CH_3 plus H_2O. (b) Space-filling representation of $[Co_4(OCH_3)_8]^-$. Co: large, O: black, C: grey, H: white. Conformational variability is possible for Co–OCH_3.

3.7. Reactions of $[CoO_2]^-$ and $[Co_4O_4]^-$ with H_2S, N_2O, and D_2O

$[CoO_2]^-$ reacted with H_2S to produce abundant HS^-, and much less $[CoO_2H]^-$. Also formed with low intensities were S_3^-, $[CoOSH]^-$, $[CoO_2S]^-$ (and/or $[CoS_2]^-$) and $[CoO_2SH]^-$ (and/or $[CoS_2H]^-$). Reaction of $[Co_4O_4]^-$ with H_2S yielded mainly HS^-, together with substitution/addition products $[Co_4O_3S]^-$, $[Co_4O_2S_2]^-$ (and/or $[Co_4O_4S]^-$), $[Co_4OS_3]^-$ (and/or $[Co_4O_3S_2]^-$). $[CoO_3]^-$ was formed by reaction of $[CoO_2]^-$ with N_2O, while $[Co_4O_4]^-$ plus N_2O yielded $[Co_4O_{4+n}]^-$, $n = 1$–3.

The products of reaction of D_2O with $[CoO_2]^-$ and $[Co_4O_4]^-$ are listed in Table 6. The principal processes are addition of OD and addition of O. Abundant products are $[CoO_3]^-$, $[Co_4O_4(OD)]^-$, and $[Co_4O_8]^-$, the latter being the most intense peak over a time period of 7–80 s. General development of OD ligands is not evident, and the typical product $[CoO_3D_4]^-$ probably contains coordinated OD_2.

Table 6
Anions produced by the reactions of $[CoO_2]^-$ and $[Co_4O_4]^-$ with D_2O

$[Co_4O_4]^-$			$[CoO_2]^-$		
Mass	Intensity (%)	Formula	Mass	Intensity (%)	Formula
32	65	O_2	32	20	O_2
35	70	H_3O_2/DHO_2	107	100	CoO_3
91	35	CoO_2	115	15	CoO_3D_4
107	35	CoO_3			
166	5	Co_2O_3			
318	100	Co_4O_5D			
332	4	Co_4O_6			
350	6	Co_4O_7D			
354	15	$Co_4O_7D_3$[a]			
364	100	Co_4O_8			
366	75	Co_4O_8D[b]			
368	5	$Co_4O_8D_4$[b]			

[a] Ion observed only in some spectra.
[b] Ion observed only in a few spectra where $[Co_4O_8]^-$ was not observed.

4. Discussion

We have described the formation of $[Co_xO_y]^-$ clusters ranging in size up to $[Co_{13}O_{14}]^-$, with the general formulas $[Co_xO_x]^-$ and $[Co_xO_{x+1}]^-$, and with the equiatomic series more abundant. The clusters with $x > 6$ occur with low abundance, and this is consistent with a previous investigation which reported species only up to $[Co_6O_7]^-$ [11]. Three ions, $[CoO_2]^-$, $[Co_2O_3]^-$ and $[Co_4O_4]^-$, are prominent in both studies.

4.1. Structure

There is limited information about the possible structures of these clusters. We have been able to achieve collision-induced dissociation for $[Co_xO_x]^-$ for $x = 5$, but apart from confirming the stability of $[CoO_2]^-$ and $[Co_4O_4]^-$ these results provide little insight into structure other than to be consistent with a cubanoid structure for $[Co_4O_4]^-$. We note that the CID of cationic $[Co_xO_y]^+$ clusters yielded generally CoO loss for $y = x$, and Co loss for $y = x + 1$ [18]. The CID of $[Co_2O_3]^-$ is consistent with the extended connectivity [O–Co–O–Co–O]$^-$, but general experience and theoretical investigations of clusters with composition M_2E_3 (E = O, S, P) leads to the expectation of a more compact structure with additional bonds. Some preliminary density functional calculations indicate that [O–Co–O]$^-$ has a flat potential energy surface, and that $[Co_4O_4]^-$ probably has a complex electronic structure, which is relatively electron rich. The assumed cubanoid structure **1** is supported by the CID results and by the consistent structural and mechanistic interpretation it enables for the reactions with alcohols.

The pattern in the compositions of the $[Co_xO_y]^-$ clusters closely matches that of the $[Mn_xS_y]^-$ and $[Mn_xS_xO]^-$ clusters [4,19]. Therefore, it is possible that the extensive density functional calculations on $[Mn_xS_y]^-$ species, and at least some of the structural conclusions, would be transferable to the $[Co_xO_y]^-$ series. This is still to be tested, but it does provide a good starting point for consideration of the structures of $[Co_xO_y]^-$. Clearly an $[Mn_xS_x]^-$ series and a $[Co_xO_x]^-$ series are not isoelectronic, and this draws attention to the evident different electron population patterns (or electron counting rules) for metal oxide anionic clusters and metal sulfide anionic clusters. The electron population per metal in $[M_xE_y]^-$, which we have evaluated as $N_m = \{x(\text{number of 3d and 4s electrons in } M^0) + 6y + 1\}/x$

[2], tends to a value of $N_m = 12$–13 for E = S as x increases, and to a higher value of $N_m = 15$–16 for E = O [11]. The fundamental reasons for this are not yet identified. Since all of these species are observed as anions in the gas phase, it is possible that this difference in electron population between oxides and sulfides is related to the electron affinities of the clusters [19].

The largest cobalt oxide cluster observed, $[Co_{13}O_{14}]^-$, possibly has the structure **5** of the unit cell of NaCl, a high symmetry fragment of the cubic close packed array.

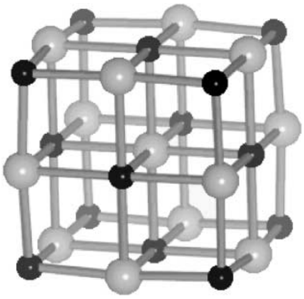

$[Co_{13}O_{14}]^-$ **5**

4.2. Reactions with alcohols

The two most prominent ions, $[CoO_2]^-$ and $[Co_4O_4]^-$, undergo extensive reactions with methanol, ethanol, and 2-propanol. The major reaction pathway for $[CoO_2]^-$ is dehydrogenation of the alcohol, and formation of $[CoO_2H]^-$ and $[CoO_2H_2]^-$. The oxidation products of the alcohols are neutral and not observed. This is consistent with the general oxidising power of $[MO_2]^-$ where the formal oxidation state is M(III), and has been similarly observed with other M [11,12,20]. It is possible and probable that $[CoO_2]^-$ also deprotonates alcohols, forming unobservable $[CoO_2H]$, because we find that $[CoO_2]^-$ deprotonates acetone and H_2S. The non-observation of alkoxides OR^- could be due to their further rapid oxidation. There is some conversion of $[CoO_2]^-$ to $[CoO_3]^-$ by alcohols, as observed previously [11]. New species observed here in the reactions of $[CoO_2]^-$ are the low abundance mono-cobalt alkoxides $[OCo(OR)_2]^-$ and $[Co(OR)_3]^-$ (for R = Me, Et, 2-Pr), and $[OCo(OH)(OR)]^-$ and $[CoO_2(R–H)]^-$ (for R = Et and 2-Pr). Our experiments have revealed a number of mono-cobalt species not seen in the previous investigations of $[CoO_2]^-$ with methanol [11].

Metal alkoxide formation is the dominant process in the reactions of $[Co_4O_4]^-$ with alcohols. There is no evidence of species such as $[Co_4O_4H]^-$ or $[Co_4O_4H_2]^-$ which would indicate dehydrogenation of alcohols, in contrast to the behaviour of $[CoO_2]^-$, and this is consistent with the expected lower oxidising ability of $[Co_4O_4]^-$.

There is a well-defined pattern of reactions of $[Co_4O_4]^-$ with alcohols (Scheme 1). There are two basic processes; (a) addition of ROH to convert μ_3–O to μ_3–OH and add OR to Co, and (b) addition of ROH across μ_3–OH, eliminating water and forming μ_3–OR (Fig. 4). Process (b) is generally faster than (a). The net effect of (a) + (b) is conversion of a (μ_3–O)–Co section of the cluster to (μ_3–OR)–CoOR (Scheme 1, Fig. 3). With the proposed cubanoid structure of $[Co_4O_4]^-$ this process can occur four times, and it does, leading eventually to the homoleptic cobalt alkoxide $[Co_4(OR)_8]^-$ (**4**). There is no evidence for elimination of H_2O from two μ_3–OH in intermediates, which is consistent with the separation of such OH in the cubanoid structures and the maintenance of the cubane core. Similarly there is no evidence for elimination of ether ROR from two μ_3–OR or from μ_3–OR and Co–OR, and diethyl ether does not react with $[Co_4O_4]^-$. Of the possible types of reactions between $[Co_4O_4]^-$ and ROH, namely oxidation of ROH, coupling ROH with elimination of water, and cobalt alkoxide formation, only the latter occurs.

We consider that the formation of the homoleptic cobalt alkoxide $[Co_4(OR)_8]^-$ as a stable and abundant product in the gas phase is a significant result. Fig. 5 shows a computer-modelled structure for the bulkiest species, $[Co_4(O–2\text{-}Pr)_8]^-$. There is limited information in the literature on the gas phase chemistry of homoleptic metal alkoxides—recent papers deal with $Ti(OR)_4$ [21], and $Ge(OCH_3)_4$ and

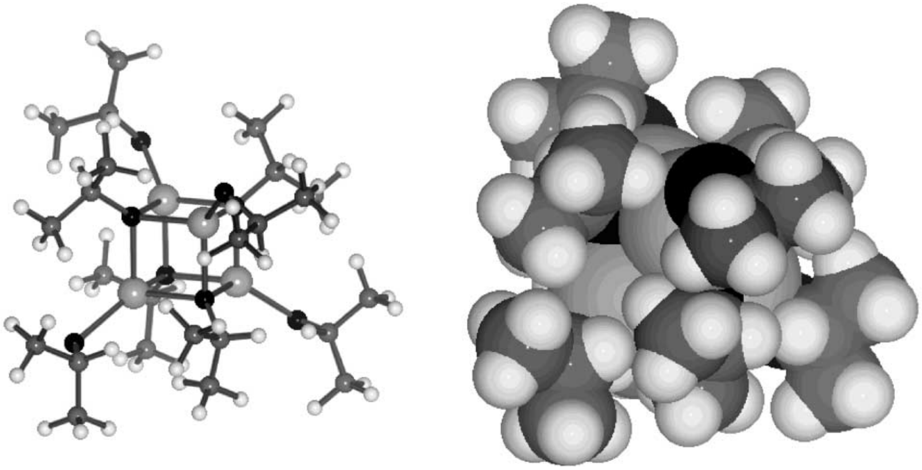

Fig. 5. Skeletal and space-filling representations of $[Co_4\{OCH(CH_3)_2\}_8]^-$. Co: large, O: black, C: grey, H: white. Considerable conformational variation is possible in the μ_3–$OCH(CH_3)_2$ and Co–$OCH(CH_3)_2$ ligands.

$[Ge(OCH_3)_4]^-$ [22]—but the species $[Co_4(OR)_8]^-$ and $[Co(OR)_3]^-$ appear to be unique. It is our hypothesis that $[Co_4(OR)_8]^-$ forms because the anionic oxide that reacts with the alcohol is not oxidising, and therefore we expect that other metal oxide anions in low formal oxidation states will similarly react with alcohols to generate homoleptic metal alkoxides by similar reactions. The larger $[Co_xO_y]^-$ ions observed here could be suitable if they can be generated with sufficient abundance, as would, for example, $[Zn_xO_y]^-$ clusters. A similar investigation of the reactions of $[Nb_xO_y]^-$ clusters with alcohols [14], $[Nb_3O_8]^-$ reacted with four molecules of methanol but the larger cluster $[Nb_4O_{10}]^-$ was unreactive with alcohols. Detailed investigations of the reaction of oxidising $[Mo_2O_7]^{2-}$ with primary alcohols reveal the oxidative mechanism [15].

Reactions believed to be homologation of coordinated methoxide to coordinated ethoxide by further slow reaction of $[Co_4(OCH_3)_8]^-$ with methanol have been observed. Water is eliminated. We are not aware of other such reactions observed in the gas phase.

The ability to generate gaseous homoleptic metal alkoxides, as anions controllable by ion optical techniques, or as neutral species by electron abstraction from these anions, could be valuable in the chemical vapour deposition processes involving these metals.

Acknowledgements

This research was supported by the Australian Research Council (ARC) and the University of New South Wales. MNY thanks the ARC for financial support during her Ph.D. studies, and acknowledges the assistance of Professors Robert N. Lamb and D. Brynn Hibbert with this publication.

References

[1] I.G. Dance, K.J. Fisher, Prog. Inorg. Chem. 41 (1994) 637;
I.G. Dance, K.J. Fisher, Mater. Sci. Forum 152 (1994) 137.

[2] K.J. Fisher, I.G. Dance, G.D. Willett, M. Yi, J. Chem. Soc., Dalton Trans. (1996) 709.

[3] J.H. El Nakat, I.G. Dance, K.J. Fisher, D. Rice, G.D. Willett, J. Am. Chem. Soc. 113 (1991) 5141;
J.H. El Nakat, K.J. Fisher, I.G. Dance, G.D. Willett, Inorg. Chem. 32 (1993) 1931;
K.J. Fisher, I.G. Dance, G.D. Willett, Polyhedron 16 (1997) 2731;
M. Yi, K. Fisher, I.G. Dance, New J. Chem. 25 (2001) 73.

[4] I.G. Dance, K.J. Fisher, G.D. Willett, J. Chem. Soc., Dalton Trans. (1997) 2557.

[5] L. Sallans, K.R. Lane, B.S. Freiser, J. Am. Chem. Soc. 111 (1989) 865.

[6] W.J. Miller, J. Chem. Phys. 57 (1972) 2354;
D.L. Bricker, D.H. Russell, J. Am. Chem. Soc. 109 (1987) 3910;
E.B. Rudny, L.N. Sidorov, L.A. Kuligina, G.A. Semenov, Int. J. Mass Spectrom. 64 (1985) 95.

[7] J.L. Franklin, J.L. Wang, J.L. Margrave, J. Inorg. Nucl. Chem. 37 (1974) 1107.

[8] R.R. Squires, J. Am. Chem. Soc. 106 (1984) 2719.

[9] R.R. Squires, Chem. Rev. 87 (1987) 623.

[10] C.J. Cassady, S.W. McElvany, in: Proceedings of the ASMS Conference on Mass spectrometry and Allied Topics, May, Miami Beach, FL, 1989, p. 161.

[11] M.C. Oliveira, J. Marcalo, M.C. Viveira, M.A. Almoster-Ferreira, Int. J. Mass Spectrom. 825 (1999) 185–187.

[12] R.H. Fokkens, I.K. Gregor, N.M.M. Nibbering, Rapid Commun. Mass Spectrom. 5 (1991) 368.

[13] R.H. Fokkens, I.K. Gregor, N.M.M. Nibbering, Org. Mass Spectrom. 27 (1992) 1013.

[14] P. Jackson, K.J. Fisher, G.D. Willett, Chem. Phys. 262 (2000) 179.

[15] T. Waters, R.A.J. O'Hair, A.G. Wedd, Chem. Commun. (2000) 225.

[16] B. Delley, New J. Chem. 16 (1992) 1103;
B. Delley, in: J.M. Seminario, P. Politzer (Eds.), Modern Density Functional Theory: A Tool for Chemistry, Vol. 2, Amsterdam, Elsevier, 1995, p. 221.

[17] M.N. Yi, Ph.D. Thesis, University of New South Wales, 1998.

[18] R.B. Freas, B.I. Dunlap, B.A. Waite, J.E. Campana, J. Chem. Phys. 86 (1987) 1276.

[19] I.G. Dance, K.J. Fisher, J. Chem. Soc., Dalton Trans. (1997) 2563.

[20] M.C. Oliveira, J. Margalo, M.C. Vieira, M.A. Almoster-Ferreira, Adv. Mass Spectrom. 14 (1998) 1.

[21] S.M. Damo, K.-C. Lam, A. Rheingold, M.A. Walters, Inorg. Chem. 39 (2000) 1635.

[22] N.H. Morgon, L.A. Xavier, J.M. Riveros, Int. J. Mass Spectrom. 195/196 (2000) 363.